ELSEVIER

PII: S0142-9612(97)00073-2

Biomaterials **18** (1997) 1325–1330

0142-9612/97/$17.00

Elastic properties of human cortical and trabecular lamellar bone measured by nanoindentation

Jae-Young Rho, Ting Y. Tsui* and George M. Pharr*

*Department of Biomedical Engineering, University of Memphis, Memphis, TN 38152, USA; *Department of Materials Science, Rice University, Houston, TX 77005-1892, USA*

An experimental investigation was undertaken to measure the intrinsic elastic properties of several of the microstructural components of human vertebral trabecular bone and tibial cortical bone by the nanoindentation method. Specimens from two thoracic vertebrae (T-12) and two tibiae were obtained from frozen, unembalmed human male cadavers aged 57 and 61 years. After drying and mounting in epoxy resin, nanoindentation tests were conducted to measure Young's modulus and the hardness of individual trabeculae in the vertebrae and single osteons, and interstitial lamellae in the tibiae. Measurements on the vertebral trabeculae were made in the transverse direction, and the average Young's modulus was found to be 13.5 ± 2.0 GPa. The tibial specimens were tested in the longitudinal direction, yielding moduli of 22.5 ± 1.3 GPa for the osteons and 25.8 ± 0.7 GPa for the interstitial lamellae. Analysis of variance showed that the differences in the measured moduli are statistically significant. Hardness differences among the various microstructural components were also observed.

Keywords: Nanoindentation, Young's modulus, hardness, trabecular bone, osteons, interstitial lamellae

Received 21 January 1997; accepted 11 April 1997

The elastic properties of bone have been measured at the microstructural level in many investigations[1–14]. Some of the microstructural features of interest include individual trabeculae[1–8], single osteons[9–11] and the thin cortical shell[12–14]. For many years, it was assumed that the elastic moduli of these microstructural components are similar to those of dense cortical bone. However, recent investigations have suggested that this may not be the case; rather, the moduli of some of the components may be smaller[1–14]. In addition, it appears that significant variations in Young's modulus may exist within a given microstructural component; for example, Young's moduli for individual trabeculae reported in the literature range from 1 to 14 GPa[1–8]. It should be noted, however, that even the largest of these values is still smaller than the frequently quoted modulus for dense cortical bone, $E = 17.1$ GPa[15].

Observations of specimen size influences on the measured modulus also suggest that the elastic moduli of the individual microstructural components of bone may not be the same as the macroscopically measured values. Choi *et al.*[2] found that Young's modulus for cortical bone measured in micro-bending tests decreases with decreasing specimen size. In separate studies, Choi *et al.*[2] and Lotz *et al.*[13] found that Young's modulus for cortical bone obtained from micro-bending tests (5.4 and 12.5 GPa, respectively) is considerably smaller than that obtained by others in tensile tests of large specimens (17.1 GPa)[15]. One explanation for these observations is that the elastic properties of the microstructural components of bone are not the same as the macroscopic values. In this regard, a technique by which the elastic properties of the individual microstructural components can be measured would be of great value in understanding the mechanical behaviour of bone at the microstructural level.

Nanoindentation is one such technique. Developed over the last 10 years, nanoindentation is now used widely in the materials science community for probing the mechanical properties of thin films, small volumes and small microstructural features[16]. The properties most commonly measured are Young's modulus, E, and hardness, H[16,17]. One of the great advantages of the technique is its ability to probe a surface and map its properties on a spatially-resolved basis, often with a resolution of better than 1 μm. Since many of the microstructural features of interest in bone are several micrometres or more in dimension, the nanoindentation technique offers a means by which their intrinsic mechanical properties can be measured directly. In the present study, the nanoindentation method was used to determine the elastic modulus, and hardness of individual vertebral trabeculae and single osteons and interstitial lamellae in tibial cortical bone.

Correspondence to Dr J.-Y. Rho.

MATERIALS AND METHODS

Two thoracic vertebrae (T-12) and two tibiae were obtained from two frozen, unembalmed human male cadavers 57 and 61 years of age (one vertebra and one tibia from each cadaver). For the vertebrae, the spinous processes were first removed, and the vertebral body was cut to a thickness of 2 mm along the sagittal plane with a low-speed diamond saw (Buehler Isomet 1000, Buehler, Lake Bluff, IL, USA) under constant deionized water irrigation. Each section was obtained from the anterior aspect. Following removal of the bone marrow using a water jet (Teledyne Water Pic, Fort Collins, CO, USA), the sections were dehydrated in a series of alcohols to avoid problems that can be caused by surface liquid films in identifying the point of first contact during indenter approach to the specimen surface. With machine and software modifications currently under development, such problems can potentially be overcome in future work, and it may be possible to test wet as well as dry specimens. Influences of specimen dehydration on nanoindentation property measurement will be discussed in the next section.

After dehydration, the specimens were embedded in epoxy resin (Epo-Thin™ low viscosity epoxy; Buehler) to provide support for the porous network and then metallographically polished to produce the smooth surfaces needed for nanoindentation testing, first with silicon carbide abrasive papers of decreasing grit size (600, 800 and 1200 grit), and finally with diamond suspensions (0.3 and 0.05 μm particle size) embedded in soft polishing cloths. The specimens were washed in deionized water between each polishing step to remove debris, taking care that the surface of the bone was not demineralized. The polished surfaces of the vertebral sections were oriented such that nanoindentation testing measured their properties in the transverse direction. Longitudinal properties were not measured due to difficulties in finding and unambiguously identifying the individual lamellae in the polished sections. Sections of the tibiae were prepared in a similar fashion, but with the specimen oriented for measurements in the longitudinal direction, for which individual osteons and trabeculae were easy to identify.

All experiments were performed using the Nano Indenter II (Nano Instruments, Inc., Knoxville, TN, USA) at the Oak Ridge National Laboratory. This fully automated hardness testing system makes small indentations at precise positions on a surface while continuously monitoring the loads and displacements of the indenter with resolutions of 0.3 μN and 0.16 nm, respectively. A sharp Berkovich diamond indenter, a three-sided pyramid with the same area-to-depth ratio as the Vickers indenter used commonly in conventional microhardness testing, was used for all measurements. In a typical experiment, the microstructural feature to be examined was located in the microscope and positioned beneath the indenter using the x–y table. The indenter was then slowly driven toward the surface at a constant displacement rate of 10 nm s^{-1} until surface contact was detected by changes in the load and displacement signals. After contact, a permanent hardness impression was made by driving the indenter into the specimen to a depth of 1000 nm at a constant loading rate of 750 μN s^{-1}, holding at this load for a period of 10 s and then unloading to 15% of the peak load at a rate equal to half that used during loading. At the end of the unloading cycle, the indenter was held on the surface for a period of 100 s to establish the rate of thermal drift in the machine and specimen for correction of the data, and then completely withdrawn. Approximately five indentations were made in each feature. Any indentations close to the mounting resin were removed from the data set to minimize effects of embedding on the measurements.

The indentation load–displacement data obtained in these tests were analysed to determine the hardness, H, and Young's modulus, E, using the method of Oliver and Pharr[18]. The first step in the analysis procedure is to determine the contact stiffness, S, a measure of the resistance of the bone to elastic deformation. As shown in the schematic depiction of a typical indentation load–displacement curve during one cycle of loading and unloading in *Figure 1*, the contact stiffness is experimentally measured from the load–displacement data as the slope of the upper portion of the unloading curve. Young's modulus is related to the contact stiffness by

$$S = \frac{2}{\sqrt{\pi}} \beta \left(\frac{1 - \nu_b^2}{E_b} + \frac{1 - \nu_i^2}{E_i} \right)^{-1} \sqrt{A} \quad (1)$$

where E_b and ν_b are Young's modulus and Poisson's ratio, respectively, for the bone, E_i and ν_i are the same quantities for the indenter, and the factor β is a constant which depends on the indenter geometry. For the Berkovich indenter, $\beta = 1.034$. This equation is derived under the assumption that the material is homogeneous and isotropic in its elastic properties. When used to measure the elastic modulus of an anisotropic material, the modulus derived from

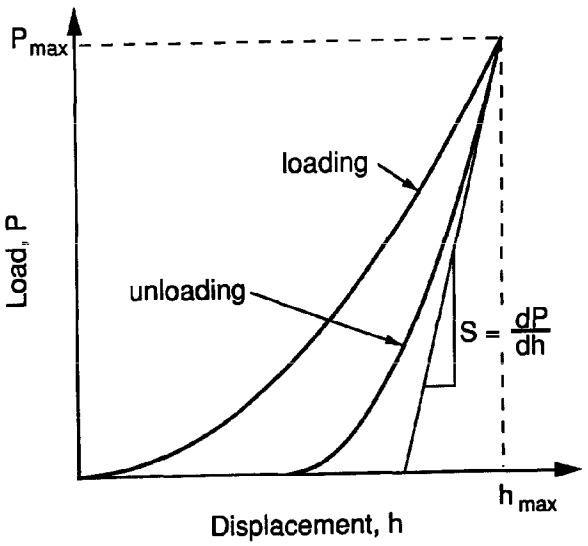

Figure 1 A schematic illustration of typical indentation load–displacement behaviour during one cycle of loading and unloading, showing quantities used to determine hardness and Young's modulus from the data. The quantities are the peak indentation load, P_{max}, the maximum indenter displacement, h_{max}, and the initial unloading stiffness, S.

Equation 1 is an average of the anisotropic elastic constants which is biased toward the modulus in the direction of testing[19,20]. If the elastic symmetry of the material is known, it is possible to perform experiments to determine the individual anisotropic elastic constants. However, in this paper, only the simple average value is reported. For a diamond indenter, $E_i = 1141\,\text{GPa}$ and $\nu_i = 0.07$, and we assume that Poisson's ratio for bone is $\nu_b = 0.3$[15]. A sensitivity study showed that varying ν_b in the range 0.2–0.4 changed the measured values of E_b by no more than 8%.

The use of *Equation 1* in the measurement of elastic modulus requires an independent measure of the contact area, A. As detailed elsewhere[18], the contact area can be estimated directly from the indentation load–displacement data through a process which requires a precise knowledge of the shape of the indenter determined in special calibration experiments and measurement of the 'plastic depth' of the contact, also referred to as the 'contact depth'. The contact depth can be computed from the contact stiffness, S, the peak load, P_{max}, and the maximum depth of penetration, h_{max}, all of which are experimentally measurable from the load–displacement data. The hardness, H, which physically represents the mean pressure the material can support, can also be determined from this procedure. The hardness is defined as the maximum load, P_{max}, divided by the projected area of the contact impression, A, i.e.

$$H = \frac{P_{max}}{A} \tag{2}$$

Determining the contact area in this way has the advantage that both E and H can be measured in one simple test. In addition, mechanical property measurements can be made without having to imagine the indentation. In metals and ceramics, it is not uncommon for E and H to be measured using indentations only tens of nanometres deep[18].

A total of 199 indentations were produced in the study. In the vertebrae, three to eight indentations were made in 14 separate trabeculae. For the tibiae, 12 osteons and six interstitial lamellae were tested using three to five indentations in each osteon and five to 10 indentations in each interstitial lamella. Significant differences in the elastic properties of trabeculae, osteons and interstitial lamellae were analysed using one-way analysis of variance (ANOVA). Scheffé's test was then employed to find differences between the elastic properties of the vertebral trabeculae and dense tibial cortical bone (osteons and interstitial lamellae).

A fused silica calibration standard was tested to check on the quality of the measurements. Fused silica is often used for calibration in nanoindentation testing because its relatively low modulus-to-hardness ratio, E/H, leads to a large amount of elastic recovery during unloading, and this improves measurement accuracy[18]. The elastic modulus of the fused silica sample was measured to be $71.8 \pm 0.4\,\text{GPa}$, which is within 0.3% of the known value, 72.0 GPa. This provides some assurance that the machine was properly calibrated and the analysis procedures were properly implemented.

RESULTS

Figure 2 is an optical micrograph of a linear array of nanoindentations made in one of the tibiae, illustrating how both osteons and interstitial lamellae can be individually sampled. The indentations shown in the figure are approximately 1 μm deep and 5 μm on an edge. A typical set of load–displacement data for an osteon is shown in *Figure 3*. The general shapes of the loading and unloading curves are similar to those observed in metals and ceramics[18].

A summary of the elastic moduli and hardness for the various microstructural components of the vertebrae and tibiae is presented in *Table 1*. All data in the table were obtained at an indentation depth of about 1000 nm (1 μm). It is important to remember that measurements on the trabecula were made in the transverse direction, while those on the cortical bone were in the longitudinal direction. Also included in

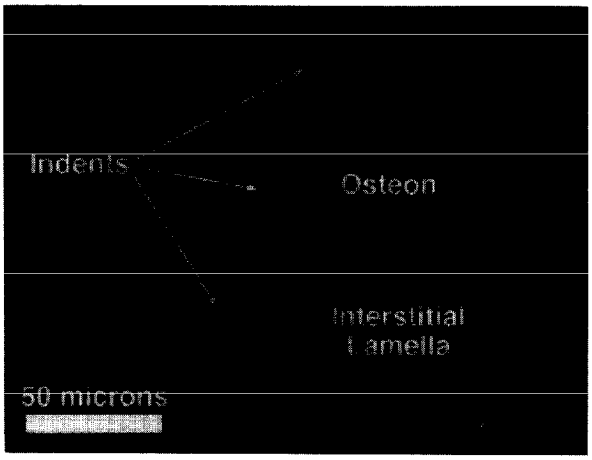

Figure 2 An optical micrograph of a linear array of nanoindentations in tibial cortical bone. Some indentations are located in an osteon while others are in an adjacent interstitial lamella.

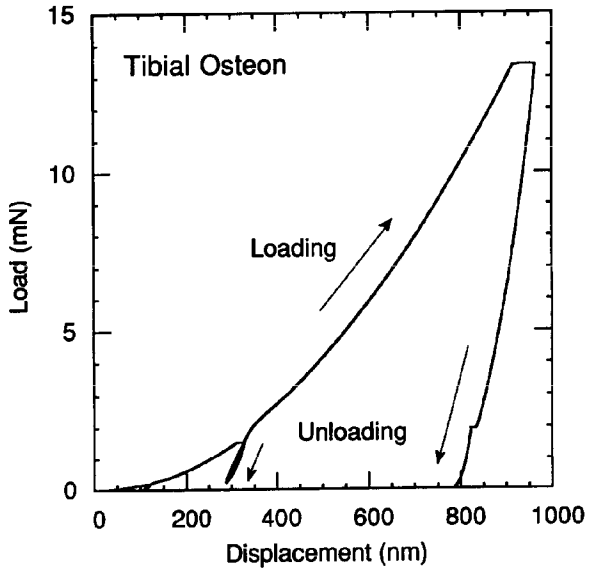

Figure 3 Load–displacement data from a nanoindentation test in a tibial osteon.

Table 1 Elastic moduli and hardnesses for the various bone microstructural components

Bone type; feature	Specimen	Number of indentations	Elastic modulus (GPa)	Hardness (MPa)
Trabecular; individual T-12 trabecula tested in transverse direction	Male age 61 (no. 8802)	8	11.1	397
		4	14.3	441
		3	15.5	490
		7	15.5	568
		5	11.6	418
		5	13.5	470
		5	13.9	485
		5	14.0	504
	Male age 57 (no. 8812)	5	8.2	262
		5	12.5	489
		5	12.7	436
		5	14.7	589
		5	14.0	515
		5	15.5	494
		Average	13.4 (2.0)	468 (79)
Cortical; tibial osteons tested in longitudinal direction	Male age 61 (no. 8802)	3	22.1	579
		4	21.7	589
		5	21.5	570
		5	20.5	527
		5	23.9	648
		5	25.0	666
		5	24.3	671
		5	23.0	610
		5	23.1	633
	Male age 57 (no. 8812)	10	21.2	622
		10	22.1	637
		10	22.0	613
		Average	22.5 (1.3)	614 (42)
Cortical; tibial interstitial lamellae tested in longitudinal direction	Male age 61 (no. 8802)	5	26.6	764
		10	25.9	741
		10	25.5	739
	Male age 57 (no. 8812)	10	26.2	761
		10	25.8	739
		10	24.6	671
		Average	25.8 (0.7)	736 (34)

Standard deviations (s.d.) are shown in parentheses.

the table are the values of E and H for each microstructural component averaged over all indentations in both specimens. The average results show that Young's modulus is greatest for the tibial interstitial lamellae ($E = 25.8$ GPa), followed in decreasing order by the tibial osteons ($E = 22.5$ GPa) and the vertebral trabeculae ($E = 13.4$ GPa). The hardnesses follow in the same order; the hardest component is the tibial interstitial lamellae ($H = 736$ MPa), followed by the tibial osteons ($H = 614$ MPa) and the vertebral trabeculae ($H = 468$ MPa). ANOVAs showed that the mean values of E and H are statistically different ($P < 0.0001$) for all the bone components.

DISCUSSION

The nanoindentation technique has several advantages over conventional microhardness measurement methods, such as the Vickers and Knoop techniques. The major benefits accrue from the accurate positioning capability (better than 1 μm) and the high resolution load and depth-sensing capabilities which enable relatively small areas of material to be tested and measured. Also, unlike conventional microhardness testing, it is not necessary for the area of nanoindentations to be optically measured in order for the hardness or elastic modulus to be determined. In this way, indentations smaller than the limit of optical resolution can be used in the testing[21], and very small features can be explored. In this study, osteons, interstitial lamellae and individual trabeculae with characteristic dimensions of tens to hundreds of micrometres were examined[22,23].

The average Young's modulus for vertebral trabeculae measured in this study, $E = 13.4$ GPa, is considerably smaller than that for the components of dense cortical bone, i.e. $E = 22.4$ GPa for osteons and $E = 25.8$ GPa for interstitial lamellae. However, some caution should be exercised in interpreting this result, since Young's moduli for the trabeculae were measured in the transverse direction, while those for the cortical bone (tibial osteons and interstitial lamellae) were measured in the longitudinal direction. In this context, it is notable that Roy *et al.*[24], using nanoindentation methods similar to those employed here, recently characterized both the transverse and the longitudinal moduli of single trabeculae and found a significant elastic anisotropy. The transverse modulus measured for horizontally-oriented trabeculae, 16.0 GPa, is similar to that measured here. However, the modulus they found in the longitudinal direction 22.7 GPa, is significantly higher, and in fact is very similar to the current measurements for tibial osteons. Thus, when

elastic anisotropy is taken into account, the differences in moduli between trabecular and cortical specimens measured in this study may not be as significant as they first appear.

In combination with the results of Roy *et al.*[24], the nanoindentation results obtained here suggest that the moduli of individual trabeculae are significantly greater than the widely used value, $E = 5.4$ GPa, obtained by microbending testing[2]. Some of this discrepancy could be due to the drying of the specimens prior to the nanoindentation testing. To estimate how large this effect might be, it is useful to refer to the work of Townsend and Rose[8], who found that drying increases Young's moduli of individual trabeculae by about 24%. Assuming this same factor applies to the nanoindentation measurements, the transverse modulus for individual trabeculae measured in this study would be about 10.2 GPa after approximate correction for the effects of drying, and the longitudinal modulus reported by Roy *et al.*[24] would correct to about 18.3 GPa. Thus, even when drying is taken into account, the nanoindentation results still suggest a higher modulus for trabeculae than what is usually assumed based on microbend testing. The reason for this discrepancy is not clear, but it could arise from difficulties encountered in making accurate mechanical property measurements with small bend specimens. These problems include: (1) influences of microstructural defects such as cement lines and voids (Haversian and Volkmann canals, lacuna, osteocytes, canaliculi and so on) on the measured displacements: (2) uncertainties in specimen geometry, which are often exacerbated at small scales; and (3) problems in properly seating and aligning small bend specimens in small test fixtures. These problems are largely avoided by the nanoindentation method, since testing can be done in areas specifically chosen to avoid defects, the test geometry is determined by the shape of an accurately calibrated diamond indenter, and seating problems are minimized through well-developed surface contact detection schemes built into the software that control the nanoindentation testing system. It is thus suggested that the inherent modulus of individual trabeculae may be considerably higher than is commonly believed.

Another question which arises is the extent to which embedding in epoxy affects the nanoindentation measurements. To minimize these effects, indentations close to the bone–resin interface were not included in the data set. Some insight into this problem can be gained from the work of Evans *et al.*[25], in which a 4% difference in hardness between embedded and unembedded bone was observed. However, as noted by the authors, it was not possible to separate the true effects of embedding from those caused by dehydration during the embedding process. Further studies of the effects of dehydration and specimen embedding on nanoindentation property measurement are warranted. For cortical bone, it should be feasible to make nanoindentation measurements on both wet and dry bone in both embedded and unembedded specimens and thus directly address both influences at once. On the other hand, it seems unlikely that trabecular bone can be studied without embedding, so answers to these questions may have to come from tests on cortical bone.

To the best of our knowledge, the elastic moduli of interstitial lamellae have not been measured previously. The results obtained here show that there is a statistically significant difference in Young's moduli of interstitial lamellae and osteons in the same bone, with the modulus of the interstitial lamellae being about 15% greater. Based on these observations, the modulus of a macroscopic sample of cortical bone should fall somewhere between that of the osteons and interstitial lamellae, with the exact value depending on the microstructural arrangement of the two components and their relative volume fractions. If the volume fractions were known, isostress or isostrain averages could be used to provide bounds on the macroscopic modulus. The isostrain average would probably give the better estimate, since the osteons and interstitial lamellae are arranged in the longitudinal direction in a manner which subjects them more to isostrain than isostress conditions. As to why Young's moduli of osteons and interstitial lamellae are different, it has been observed using backscattering scanning electron microscopy that interstitial bone is more mineralized than osteons[26]. The lower elastic modulus for osteons may thus result from the osteons being newer bone material than the interstitial lamellae, since newer bone is known to have lower mineral content[27]. As further support for this notion, Evans and Vincentelli[28] have reported that osteons tend to reduce both the strength and the elastic modulus of cortical bone.

This initial study demonstrates that the nanoindentation method can offer valuable insight into the elastic properties of the microstructural components of bone. Properties measured by nanoindentation could prove useful in the development of theoretical micromechanical models[29–31] and in finite element modelling. The nanoindentation characterization of the mechanical properties of bone at the microstructural level could also provide information useful in understanding the complex interactions of biological and cellular mechanisms for osseous disorders.

ACKNOWLEDGEMENTS

This research was sponsored by the Whitaker Foundation, the Oak Ridge Associated Universities Junior Faculty Enhancement Grant and a Faculty Research Grant at the University of Memphis (J.Y.R.). Instrumentation for the nanoindentation work was provided by the Division of Materials Sciences, US Department of Energy, under contract DE-AC05-96OR22464 with Lockheed Martin Energy Research Corp., and through the SHaRE Program under contract DE-AC05-76OR00033 with the Oak Ridge Institute for Science and Technology. One of the authors (G.M.P.) is grateful for sabbatical support provided by the Oak Ridge National Laboratory.

REFERENCES

1. Ashman, R. B. and Rho, J. Y., Elastic moduli of trabecular bone material. *J. Biomech.*, 1988, **21**, 177–181.
2. Choi, K., Kuhn, J. L., Ciarelli, M. J. and Goldstein, S. A., The elastic moduli of human subchondral trabecular, and cortical bone tissue and the size-dependency of cortical bone modulus. *J. Biomech.*, 1990, **23**, 1103–1113.

3. Kuhn, J.L., Goldstein, S.A., Choi, K.W., London, M., Feldkamp, L.A. and Matthews, L.S., Comparison of the trabecular and cortical tissue moduli from human iliac crests. *J. Orthop. Res.*, 1989, **7**, 876–884.
4. Mente, P.L. and Lewis, J.L., Experimental method for the measurement of the elastic modulus of trabecular bone tissue. *J. Orthop. Res.*, 1989, **7**, 456–461.
5. Rho, J.Y., Ashman, R.B. and Turner, C.H., Young's modulus of trabecular and cortical bone material: ultrasonic and microtensile measurements. *J. Biomech.*, 1993, **26**(2), 111–119.
6. Runkle, J.C. and Pugh, J., The micro-mechanics of cancellous bone. *Bull. Hosp. J. Dis.*, 1975, **36**, 2–10.
7. Ryan, J.C. and Williams, J.L., Tensile testing of rodlike trabeculae excised from bovine femoral bone. *J. Biomech.*, 1989, **22**, 351–355.
8. Townsend, P.R. and Rose, R.M., Buckling studies of single human trabeculae. *J. Biomech.*, 1975, **8**, 199–201.
9. Ascenzi, A. and Bonucci, E., The tensile properties of single osteons. *Anat. Rec.*, 1967, **158**, 375–386.
10. Ascenzi, A. and Bonucci, E., The compressive properties of single osteons. *Anat. Rec.*, 1968, **161**, 377–392.
11. Ascenzi, A., Baschieri, P. and Benvenuti, A., The bending properties of a single osteon. *J. Biomech.*, 1990, **23**, 763–771.
12. Brown, T.D. and Vrahas, M.S., The apparent elastic modulus of the juxtarticular subchondral bone of the femoral head. *J. Orthop. Res.*, 1984, **2**(1), 32–38.
13. Lotz, J.C., Gerhart, T.N. and Hayes, W.C., Mechanical properties of metaphyseal bone in the proximal femur. *J. Biomech.*, 1991, **24**, 317–329.
14. Murray, R.P., Hayes, W.C., Edwards, W.T. and Harry, J.D., Mechanical properties of the subchondral plate and the metaphyseal shell. *Trans. 30th ORS*, 1984, **9**, 197.
15. Reilly, D.T., Burstein, A.H. and Frankel, V.H., The elastic modulus of bone. *J. Biomech.*, 1974, **7**, 271–275.
16. Pharr, G.M. and Oliver, W.C., Measurement of thin film mechanical properties using nanoindentation. *MRS Bull.*, 1992, **17**(7), 28–33.
17. Doerner, M.F. and Nix, W.D., A method for determining the data from depth-sensing indentation instruments. *J. Mater. Res.*, 1986, **1**, 601.
18. Oliver, W.C. and Pharr, G.M., An improved technique for determining hardness and elastic modulus using load and displacement sensing indentation experiments. *J. Mater. Res.*, 1992, **7**(6), 1564–1583.
19. Vlassak, J.J. and Nix, W.D., Indentation modulus of elastically anisotropic half spaces. *Phil. Mag.*, 1993, **A67**, 1045–1056.
20. Vlassak, J.J. and Nix, W.D., Measuring the elastic properties of anisotropic materials by means of indentation experiments. *J. Mech. Phys. Solids*, 1994, **42**, 1223–1245.
21. Willems, G., Celis, J.P., Lembrechts, P., Braem, M. and Vanherle, G., Hardness and Young's modulus determined by nanoindentation technique of filler particles of dental restorative materials compared with human enamel. *J. Biomed. Mater. Res.*, 1993, **27**, 747–755.
22. Tao, N.J., Lindsay, S.M. and Lees, S., Measuring the microelastic properties of biological material. *Biophys. J.*, 1992, **63**, 1165–1169.
23. Hodgskinson, R., Currey, J.D. and Evans, G.P., Hardness, an indicator of the mechanical competence of cancellous bone. *J. Orthop. Res.*, 1989, **7**, 754–758.
24. Roy, M., Rho, J.Y., Tsui, T.Y. and Pharr, G.M., Variation of Young's modulus and hardness in human lumbar vertebrae measured by nanoindentation. *Adv. Bioeng.*, 1996, **BED-33**, 385–386.
25. Evans, G.P., Behiri, J.C., Currey, J.D. and Bonfield, W., Microhardness and Young's modulus in cortical bone exhibiting a wide range of mineral volume fractions, and in a bone analogue. *J. Mater. Sci.: Mater. Med.*, 1990, **1**, 38–43.
26. Dorlot, J.-M., L'Esperance, G. and Meunier, A., Characterization of single osteons: microhardness and mineral content. *Trans. 32nd Orthop. Res. Soc.*, 1986, **11**, 330.
27. Katz, J.L. and Meunier, A., Scanning acoustic microscope studies of the elastic properties of osteons and osteon lamellae. *J. Biomech. Eng.*, 1993, **115**, 543–548.
28. Evans, F.G. and Vincentelli, R., Relations of the compressive properties of human cortical bone to histological structure and calcification. *J. Biomech.*, 1974, **7**, 1–10.
29. Hogan, H.A., Micromechanics modeling of haversian cortical bone properties. *J. Biomech.*, 1992, **25**, 549–556.
30. Hollister, S.J. and Kikuchi, N., Homogenization theory and digital imaging: a basis for studying the mechanics and design principles of bone tissue. *Biotech. Bioeng.*, 1994, **43**, 586–596.
31. Pidaparti, R.M.V. and Burr, D.B., Collagen fiber orientation and geometry effects on the mechanical properties of secondary osteons. *J. Biomech.*, 1992, **25**(8), 869–880.